Analysis of a Ridge Waveguide Using Overlapping T-Blocks

Yong H. Cho and Hyo J. Eom, *Senior Member, IEEE*

***Abstract*—A T-block (TB) approach is proposed to analyze the dispersion relation of a ridge waveguide. The field representations of a TB are obtained with the Green's function and mode-matching technique. Rigorous, yet simple dispersion equations for symmetric and asymmetric ridge waveguides are presented using a superposition of overlapping TBs. The rapid convergence characteristics of the dispersion equation are illustrated in terms of the cutoff wavenumbers. A closed-form dispersion relation, based on a dominant-mode approximation, is shown to be accurate for most practical applications such as couplers, filters, and polarizer designs.**

***Index Terms*—Dispersion, Green's function, mode-matching technique, ridge waveguide, superposition.**

I. Introduction

THE propagation and coupling characteristics of a ridge waveguide have been investigated with various methods [1]–[7] because of its broad-band, low cutoff-frequency, and low-impedance characteristics compatible with a coaxial line. When the geometry of a waveguide is complicated such as a ridge waveguide, the formulation and dispersion analysis becomes naturally involved. It is, therefore, desirable to develop an analysis scheme with fast CPU time, increased accuracy, simple applicability, and wide versatility. To that end, we propose a new approach using the T-block (TB) and superposition. Based on the idea of superposition, the method of overlapping regions has been applied to solve some diffraction and waveguide problems [8], [9]. In [10], a simple and new equivalent network for a T-junction, which is similar to a TB, is presented to obtain the closed-form expression for open and slit-coupled E-plane T-junctions. In this paper, the approach of the TB and superposition is employed to divide a total region into several overlapping TBs. It is possible to represent the field within a TB in simple and numerically efficient series based on the Green's function and mode-matching method. The Green's function approach allows us to reduce the number of unknown modal coefficients and improve the convergence rate. Since the Green's function for the TB is available, the involved residue calculus, as in [7], is unnecessary, thereby increasing computational efficiency. The advantage of the TB approach lies in substantially reducing the amount of computational effort. In this paper, we will analyze the propagation characteristics of a double-ridge waveguide by utilizing the TB approach and superposition principle. It is important to note that our TB approach is applicable to other waveguide structures, whose geometry can be broken into several overlapping TBs such as the finline, shielded microstrip line, and multiconductor transmission line.

Manuscript received September 2, 2001; revised November 5, 2001.

The authors are with the Department of Electrical Engineering, Korea Advanced Institute of Science and Technology, Daejeon 305-701, Korea (e-mail: hjeom@ee.kaist.ac.kr).

Digital Object Identifier 10.1109/TMTT.2002.803449.

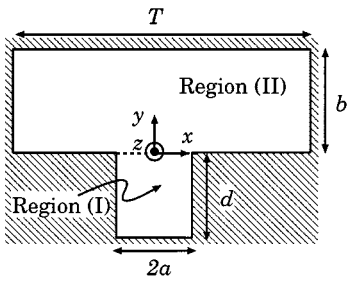

Fig. 1. Geometry of a TB.

II. Analysis of TB

Assume that a TE wave propagates along the z-direction inside a TB in Fig. 1. The phase factor $e^{j(\beta z-\omega t)}$ is omitted throughout. In region (I) ($-d < y < 0$), we represent the H_z component as

$$H_z^I(x, y) = \sum_{m=0}^{\infty} q_m \cos a_m(x+a)\cos \xi_m(y+d) \times \big[u(x+a) - u(x-a)\big] \quad (1)$$

where $a_m = m\pi/(2a)$, $\xi_m = \sqrt{k_0^2 - \beta^2 - a_m^2}$, $k_0 = 2\pi/\lambda_0$, and $u(\cdot)$ is a unit step function. In order to represent the H_z-field in region (II) ($0 < y < b$), we divide region (II) into two subregions such as shown in Fig. 2(a) and (b). Based on the superposition, the field in region (II) is given by

$$H_z^{II}(x, y) = \sum_{m=0}^{\infty} s_m \big[H_m(x, y) + R_m^H(x, y)\big] \quad (2)$$

where $H_m(x, y)$ and $R_m^H(x, y)$ are the field components within subregions of Fig. 2(a) and (b), respectively. Similar to the $H_z^I(x, y)$ component, we represent $H_m(x, y)$ as

$$H_m(x, y) = \frac{\cos \xi_m(y-b)}{\xi_m \sin(\xi_m b)} \cos a_m(x+a) \times \big[u(x+a) - u(x-a)\big]. \quad (3)$$

Multiplying the E_x-field continuity at $y = 0$ between regions (I) and (II) by $\cos a_l(x+a)$ and integrating over $-a < x < a$, we obtain

$$s_m = -q_m \xi_m \sin(\xi_m d). \quad (4)$$

The component of $H_m(\pm a, y)$ results in the H_z discontinuity at $x = \pm a$. In order to enforce the H_z continuity at $x = \pm a$,

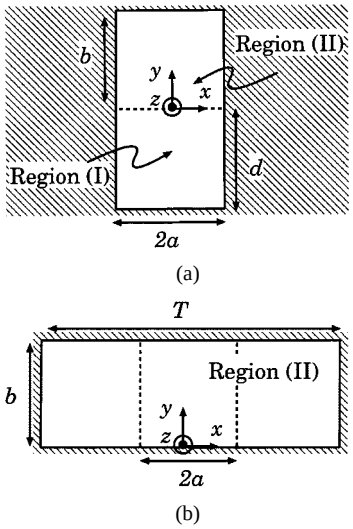

Fig. 2. Subregions of a TB. (a) Subregion for $H_m(x,\ y)$. (b) Subregion for $R_m^H(x,\ y)$.

we next consider a contribution from $R_m^H(x,\ y)$. Utilizing the Green's function relation [11] gives

$$\begin{aligned} R_m^H(x,\ y) &= \frac{1}{\mu_0}\nabla\times\overline{A}\big|_{z\ \text{component}} \\ &= -\nabla\times\int G_H(r,\ r')\overline{J}(r')\,dr'\big|_{z\ \text{component}} \\ &= -\int\frac{\partial}{\partial n}\left[G_H(r,\ r')\right]H_m(r')\,dr' \end{aligned} \tag{5}$$

where $\overline{A}$ is a magnetic vector potential, $\overline{J}(r') = H_m(r')\hat{a}_z\times\hat{n}$, n is the outward normal direction to r' in Fig. 2(a)

$$G_H(r,\ r') = \frac{2}{b}\sum_{v=0}^{\infty}\frac{\cos(\eta_v y)\cos(\eta_v y')}{\alpha_v}\,g(x,\ x';\ \zeta_v) \tag{6}$$

$$g(x,\ x';\ \zeta) = \frac{\sin\zeta(x_< + T/2)\sin\zeta(T/2 - x_>)}{\zeta\sin(\zeta T)} \tag{7}$$

$x_>\ \equiv$ is the greater of x or x', $x_<\ \equiv$ is the lesser of x or x', $\alpha_0 = 2$, $\alpha_m = 1$ $(m = 1, 2, \ldots)$, $\eta_v = v\pi/b$, $\zeta_v = \sqrt{k_0^2 - \beta^2 - \eta_v^2}$, $G_H(r,\ r')$ is shown in [11], and $g(x,\ x';\zeta_v)$ is a one-dimensional Green's function with an electric wall at $x = \pm T/2$. Note that r denotes an observation point $(x,\ y)$, and r' is a source point $(x',\ y') = (\pm a,\ 0 < y' < b)$. The scattered component $R_m^H(x,\ y)$ is thought of as the field produced to eliminate the surface current $\overline{J}(r') = H_m(r')\hat{a}_z\times\hat{n}$. This means that $R_m^H(\pm a,\ y)$ produces the $H_z(\pm a,\ y)$ discontinuity at $x = \pm a$, which is an inverse sign to $H_m(\pm a,\ y')$. Integrating (5) with respect to y' from 0 to b, we obtain

$$\begin{aligned} R_m^H(x,y) &= \int_0^b \frac{\partial G_H(r,\ r')}{\partial x}\,\frac{\cos\xi_m(y'-b)}{\xi_m\sin(\xi_m b)}\bigg|_{x'=-a}dy' \\ &\quad -(-1)^m\int_0^b\frac{\partial G_H(r,r')}{\partial x}\,\frac{\cos\xi_m(y'-b)}{\xi_m\sin(\xi_m b)}\bigg|_{x'=a}dy' \\ &= -\frac{1}{b}\sum_{v=0}^{\infty}\frac{\cos(\eta_v y)}{\alpha_v(\zeta_v^2 - a_m^2)} \\ &\quad\times\left[f_H(x,\ -a;\ \zeta_v) - (-1)^m f_H(x,\ a;\ \zeta_v)\right] \end{aligned} \tag{8}$$

where

$$f_H(x,x';\zeta) = \frac{\operatorname{sgn}(x-x')\left[e^{i\zeta|x-x'|} - (-1)^m e^{i\zeta(T-|x-x'|)}\right]}{1-(-1)^m e^{i\zeta T}} \tag{9}$$

and $\operatorname{sgn}(x) = 2u(x) - 1$. The total longitudinal magnetic field is, therefore, given as

$$T_H(x,\ y) = H_z^I(x,\ y) + H_z^{II}(x,\ y). \tag{10}$$

Note that the $E_x(x,\ 0)$-field, which is produced by $R_m(x,\ 0)$, is zero. Hence, the E_x- and H_z-field continuities are satisfied, except for the H_z-field discontinuity at $y = 0$ and $-a < x < a$. By enforcing the continuity of $T_H(x,\ 0)$ for $-a < x < a$, it is possible to determine the dispersion relation for a TB. If a waveguide structure can be divided into a number of TB, it is possible to use (10) directly in the derivation of dispersion relation. The advantage of our TB approach lies in its computational simplicity since (10) can be repeatedly used for each TB. In the following section, we will show how to obtain the dispersion relation for a ridge waveguide from (10).

Similarly from the analysis of the TE mode, the E_z components for the TM mode are represented as

$$\begin{aligned} E_z^I(x,\ y) &= \sum_{m=1}^{\infty} p_m\sin a_m(x+a)\sin\xi_m(y+d) \\ &\quad\times\left[u(x+a) - u(x-a)\right] \end{aligned} \tag{11}$$

$$E_z^{II}(x,\ y) = \sum_{m=1}^{\infty} p_m\sin(\xi_m d)\left[E_m(x,\ y) + R_m^E(x,\ y)\right] \tag{12}$$

where

$$\begin{aligned} E_m(x,\ y) &= \frac{\sin\xi_m(b-y)}{\sin(\xi_m b)}\sin a_m(x+a) \\ &\quad\times\left[u(x+a) - u(x-a)\right] \end{aligned} \tag{13}$$

$$\begin{aligned} R_m^E(x,\ y) &= -\int G_E(r,\ r')\,\frac{\partial}{\partial n'}\left[E_m(r')\right]dr' \\ &= -\frac{a_m i}{b}\sum_{v=1}^{\infty}\frac{\eta_v\sin(\eta_v y)}{\zeta_v(\zeta_v^2 - a_m^2)} \\ &\quad\times\left[f_E(x,\ -a;\ \zeta_v) - (-1)^m f_E(x,\ a;\ \zeta_v)\right] \end{aligned} \tag{14}$$

$$G_E(r,\ r') = \frac{2}{b}\sum_{v=1}^{\infty}\sin(\eta_v y)\sin(\eta_v y')g(x,\ x';\ \zeta_v) \tag{15}$$

$$f_E(x,\ x';\ \zeta) = \frac{e^{i\zeta|x-x'|} + (-1)^m e^{i\zeta(T-|x-x'|)}}{1-(-1)^m e^{i\zeta T}}. \tag{16}$$

We then obtain the total longitudinal electric field as

$$T_E(x,\ y) = E_z^I(x,\ y) + E_z^{II}(x,\ y). \tag{17}$$

Contrary to the TE mode, the total field $T_E(x,\ y)$ is continuous at $y = 0$, while the H_x-field is discontinuous. The dispersion relation can be obtained by enforcing the H_x-field continuity at $y = 0$ for $-a < x < a$. Although R_m^H and R_m^E are represented in series forms, their convergence rate is very fast, thus, efficient

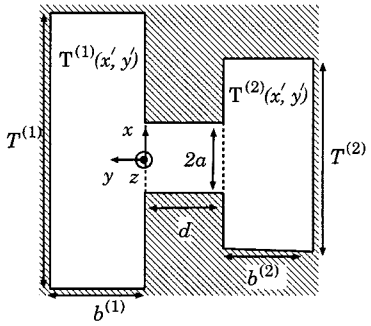

Fig. 3. Geometry of a double-ridge waveguide.

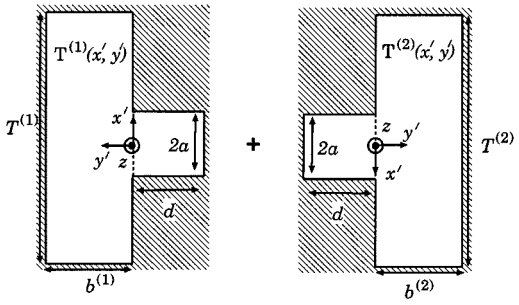

Fig. 4. Superposition of two TBs.

for numerical computations. Note that the convergence characteristics of H_z^{II} and E_z^{II} are independent of T in Fig. 1. These characteristics are different from the standard mode-matching technique, where its convergence rate is mainly determined by T. When $T \to \infty$, our solutions converge to those of a rectangular groove guide with an electric conductor cover at $y = b$ in [12].

III. Analysis of Ridge Waveguide Using Two TBs

It is possible to apply the TB approach to the dispersion analysis for a double-ridge waveguide. We first divide a double-ridge waveguide in Fig. 3 into two overlapping TBs, as shown in Fig. 4. The H_z-field in a ridge waveguide is represented as

$$H_z(x, y) = T_H^{(1)}(x, y) + T_H^{(2)}(-x, -y - d). \tag{18}$$

Note that the (x, y) coordinate in Fig. 3 is the global coordinate system for a double-ridge waveguide, and (x', y') in Fig. 4 is the local coordinate system for subregions of TBs. The enforcement of the boundary conditions on the H_z-field continuities is required to determine the relations of modal coefficients $q_m^{(1)}$ and $q_m^{(2)}$. In matching the H_z continuity, it is expedient to introduce a general integration form as

$$\begin{aligned} &I(x, y; c) \\ &\quad = \int_{x-c}^{x+c} \Big[H_z^I(x', y)\big|_{T^{(1)}+T^{(2)}} - H_z^{II}(x', y)\big|_{T^{(1)}+T^{(2)}} \Big] \\ &\qquad \times \cos c_l(x' - x + c)\, dx' \\ &\quad = \sum_{m=0}^{\infty} \Big[q_m^{(1)} I_H^{(1)}(x, y; c) + q_m^{(2)} I_H^{(2)}(-x, -y - d; c) \Big] \end{aligned} \tag{19}$$

where $c_l = l\pi/(2c)$ and

$$\begin{aligned} &I_H(x, y; c) \\ &\quad = \int_{x-c}^{x+c} \Big\{ \cos a_m(x' + a) \cos \xi_m(y + d) \\ &\qquad \times \big[u(x' + a) - u(x' - a)\big]\big[u(y + d) - u(y)\big] \\ &\qquad + \xi_m \sin(\xi_m d)\big[H_m(x', y) + R_m^H(x', y)\big] \\ &\qquad \times \big[u(y) - u(y - b)\big] \Big\} \cos c_l(x' - x + c)\, dx'. \end{aligned} \tag{20}$$

Since the integrand of $I_H(x, y; c)$ is composed of elementary functions, the evaluation of (20) is trivial. In order to satisfy the H_z continuity at $(-a < x < a, y = 0)$ and $(-a < x < a, y = -d)$, we put $(x, y) = (0, 0)$ and $(0, -d)$ into (19), respectively, and obtain the dispersion relation for a double-ridge waveguide as

$$\sum_{m=0}^{\infty} \Big[q_m^{(1)} I_H^{(1)}(0, 0; a) + q_m^{(2)} I_H^{(2)}(0, -d; a) \Big] = 0 \tag{21}$$

$$\sum_{m=0}^{\infty} \Big[q_m^{(1)} I_H^{(1)}(0, -d; a) + q_m^{(2)} I_H^{(2)}(0, 0; a) \Big] = 0. \tag{22}$$

When a double-ridge waveguide is symmetric with respect to the y-direction, $q_m^{(1)} = \pm q_m^{(2)}$. Note that $\pm$ sign denotes even and odd modes with respect to the y-direction, respectively. The dispersion equations, i.e., (21) and (22), then reduce to a simplified one as

$$\sum_{m=0}^{\infty} q_m^{(1)} \Big[I_H^{(1)}(0, 0; a) \pm I_H^{(2)}(0, -d; a) \Big] = 0. \tag{23}$$

In a dominant-mode approximation $(m = 0, l = 0)$, (23) further simplifies to

$$\begin{aligned} &I_H^{(1)}(0, 0; a) \pm I_H^{(2)}(0, -d; a)\Big|_{m=0,\, l=0} \\ &\quad = 2a\big[\cos(k_c d) \pm 1\big] \\ &\qquad + k_c \sin(k_c d) \left[\frac{2a}{k_c \tan(k_c b)} \right. \\ &\qquad\qquad \left. - \frac{2i}{b} \sum_{v=0}^{\infty} \frac{1 - e^{i\zeta_v 2a} + e^{i\zeta_v T} - e^{i\zeta_v (T-2a)}}{\alpha_v \zeta_v^3 (1 - e^{i\zeta_v T})} \right] \\ &\quad = 0 \end{aligned} \tag{24}$$

where $k_c = \sqrt{k_0^2 - \beta^2}$ and $\zeta_v = \sqrt{k_c^2 - (v\pi/b)^2}$. Similarly, utilizing the approach of TB and superposition, we obtain the TM dispersion relation of a double-ridge waveguide as

$$\sum_{m=1}^{\infty} \Big[p_m^{(1)} I_E^{(1)}(0, 0; a) - p_m^{(2)} I_E^{(2)}(0, -d; a) \Big] = 0 \tag{25}$$

$$\sum_{m=1}^{\infty} \Big[p_m^{(1)} I_E^{(1)}(0, -d; a) - p_m^{(2)} I_E^{(2)}(0, 0; a) \Big] = 0 \tag{26}$$

TABLE I
CUTOFF WAVENUMBERS (IN RADIANS PER METER) OF THE FIRST EIGHT TE MODES FOR A SINGLE-RIDGE WAVEGUIDE. PARAMETERS: $a = 1.7$ mm, $T^{(1)} = T^{(2)} = 19$ mm, $d = 0.3$ mm, $b^{(1)} = b^{(2)} = 9.35$ mm

Mode number	1	2	3	4	5	6	7	8
$m = 0$	91.34	333.1	379.9	524.7	664.7	690.5	744.8	828.0
$m = 0, 2$	92.40	333.2	380.7	525.8	665.3	692.1	745.4	828.9
$m = 0, 2, 4$	92.60	333.2	380.8	526.0	665.3	692.1	745.5	829.2
$m = 0, 2, 4, 6$	92.66	333.2	380.9	526.1	665.3	692.1	745.5	829.2
[5]	92.6	333.2	381.1	526.3	665.3	691.6	745.3	829.5

TABLE II
CUTOFF WAVENUMBERS (IN RADIANS PER METER) OF THE FIRST EIGHT TM MODES FOR A SINGLE-RIDGE WAVEGUIDE. PARAMETERS: $a = 1.7$ mm, $T^{(1)} = T^{(2)} = 19$ mm, $d = 0.3$ mm, $b^{(1)} = b^{(2)} = 9.35$ mm

Mode number	1	2	3	4	5	6	7	8
$m = 2$	471.2	471.4	741.1	741.7	748.3	748.8	940.5	942.4
$m = 2, 4$	471.1	471.4	741.0	741.7	748.2	748.8	940.3	942.3
$m = 2, 4, 6$	471.1	471.4	741.0	741.6	748.2	748.7	940.2	942.3
$m = 2, 4, 6, 8$	471.1	471.4	741.0	741.6	748.2	748.7	940.2	942.3
[5]	471.1	471.4	741.0	741.6	748.1	748.7	940.0	942.2

where

$$I(x, y; c) = \int_{x-c}^{x+c} \left[\frac{\partial}{\partial y} E_z^I(x', y)\Big|_{T^{(1)}+T^{(2)}} - \frac{\partial}{\partial y} E_z^{II}(x', y)\Big|_{T^{(1)}+T^{(2)}} \right] \times \sin c_l(x' - x + c)\, dx' = \sum_{m=0}^{\infty} \left[p_m^{(1)} I_E^{(1)}(x, y; c) - p_m^{(2)} I_E^{(2)}(-x, -y - d; c) \right] \quad (27)$$

$$I_E(x, y; c) = \int_{x-c}^{x+c} \Big\{ \sin a_m(x' + a) \sin \xi_m(y + d) \times \left[u(x' + a) - u(x' - a) \right] \left[u(y + d) - u(y) \right] - \sin(\xi_m d) \left[E_m(x', y) + R_m^E(x', y) \right] \times \left[u(y) - u(y - b) \right] \Big\} \times \sin c_l(x' - x + c)\, dx'. \quad (28)$$

In a dominant-mode approximation $(m = 2, l = 2)$ for a symmetric single-ridge waveguide, (25) and (26) reduce to

$$I_E^{(1)}(0, 0; a) \pm I_E^{(2)}(0, -d; a)\Big|_{m=2, l=2} = a\xi_2 \left[\cos(\xi_2 d) \pm 1 \right] + \sin(\xi_2 d) \cdot \left[\frac{a\xi_2}{\tan(\xi_2 b)} - \frac{2a_2^2 i}{b} \sum_{v=1}^{\infty} \frac{\eta_v^2 \left[1 - e^{i\zeta_v 2a} + e^{i\zeta_v T} - e^{i\zeta_v (T-2a)} \right]}{\zeta_v \left(\zeta_v^2 - a_2^2 \right)^2 \left(1 - e^{i\zeta_v T} \right)} \right] = 0 \quad (29)$$

where $\xi_2 = \sqrt{k_0^2 - \beta^2 - a_2^2}$. Tables I and II show the convergence characteristics of the TE and TM modes in a single-ridge waveguide, respectively. The agreement of our solution with [5] is excellent, and even a dominant-mode solution $(m = 0)$ is accurate within 1% error. This means that the dominant-mode dispersion relations, i.e., (24) and (29), are useful for most practical applications. Fig. 5 represents the cutoff wavenumber characteristics of the TE_{10} mode in a single-ridge waveguide versus the position of a ridge. As the width of the ridge d increases, the cutoff wavenumber of the TE_{10} mode decreases. This means that the bandwidth of a single-mode operation increases. The dominant-mode solution agrees well with the higher mode solutions, thus confirming the fast convergence. As $b^{(1)}/(T^{(1)} - d)$ approaches one, the solution converges to that of a single TB with $b^{(1)} = T^{(1)} - d$.

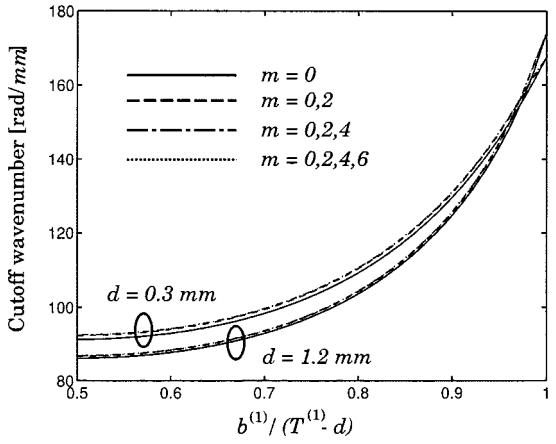

Fig. 5. Cutoff wavenumber of the TE_{10} mode in a double-ridge waveguide versus the position of the ridge. ($a = 1.7$ mm, $T^{(1)} = T^{(2)} = 19$ mm, and $b^{(1)} + b^{(2)} + d = T^{(1)}$).

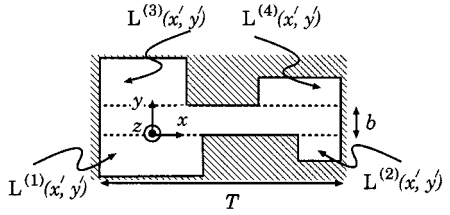

Fig. 6. Geometry of an asymmetric double-ridge waveguide.

IV. ANALYSIS OF RIDGE WAVEGUIDE USING FOUR L-BLOCKS

For the analysis of an asymmetric double-ridge waveguide in Fig. 6, it is convenient to use an L-block (LB), as shown in Fig. 7. An asymmetric double-ridge waveguide in Fig. 6 is divided into four overlapping LBs, as shown in Fig. 8. The H_z-field in an asymmetric double-ridge waveguide is represented as the superposition of four LBs. Then

$$H_z(x, y) = L_H^{(1)}(x, y) + L_H^{(2)}\left(x - T + a^{(1)} + a^{(2)}, y\right) + L_H^{(3)}\left(a^{(3)} - a^{(1)} - x, b - y\right) + L_H^{(4)}\left(T - a^{(1)} - a^{(4)} - x, b - y\right) \quad (30)$$

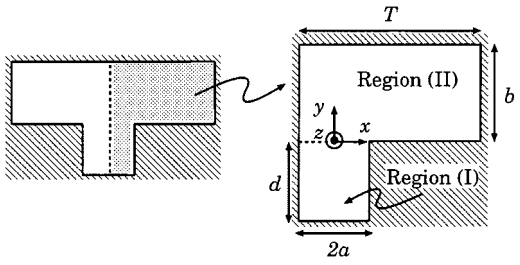

Fig. 7. Geometry of an LB.

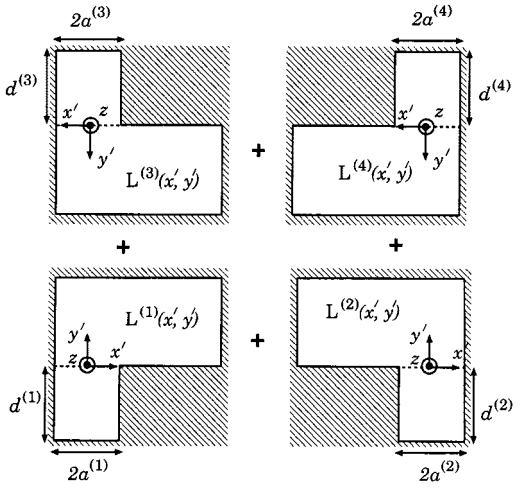

Fig. 8. Superposition of four LBs.

where $L_H(x, y) = T_H(x + a, y)|_{m=\text{even}}$. Matching points (x, y) for the H_z-field continuities are $(0,0)$, $(T - a^{(1)} - a^{(2)}, 0)$, $(a^{(3)} - a^{(1)}, b)$, and $(T - a^{(1)} - a^{(4)}, b)$ in the global coordinates of Fig. 6. Using the same procedure as in Section III, the dispersion relations of an asymmetric double-ridge waveguide are obtained. For instance, the dispersion equation corresponding to the matching point $(0,0)$ is obtained as

$$
\begin{aligned}
&I\left(0, 0; a^{(1)}\right) \\
&\quad = \int_{-a^{(1)}}^{a^{(1)}} \Big[H_z^I(x', 0)\big|_{L^{(1)}+L^{(2)}+L^{(3)}+L^{(4)}} \\
&\qquad\qquad - H_z^{II}(x', 0)\big|_{L^{(1)}+L^{(2)}+L^{(3)}+L^{(4)}}\Big] \\
&\qquad \times \cos a_l^{(1)}\left(x' + a^{(1)}\right) dx' \\
&\quad = \sum_{m=0}^{\infty} \Big[q_m^{(1)} I_{LH}^{(1)}\left(0, 0; a^{(1)}\right) \\
&\qquad\qquad + q_m^{(2)} I_{LH}^{(2)}\left(a^{(1)} + a^{(2)} - T, 0; a^{(1)}\right) \\
&\qquad\qquad + q_m^{(3)} I_{LH}^{(3)}\left(a^{(3)} - a^{(1)}, b; a^{(1)}\right) \\
&\qquad\qquad + q_m^{(4)} I_{LH}^{(4)}\left(T - a^{(1)} - a^{(4)}, b; a^{(1)}\right)\Big] \\
&\quad = 0
\end{aligned}
\tag{31}
$$

where $I_{LH}(x, y; c) = I_H(x+a, y; c)|_{m=\text{even}}$. It is straightforward to obtain the remaining three dispersion equations corresponding to $(x, y) = (T - a^{(1)} - a^{(2)}, 0)$, $(a^{(3)} - a^{(1)}, b)$, and $(T - a^{(1)} - a^{(4)}, b)$. In order to verify the validity of the approach based on the LB, in Table III we show the cutoff wavenumber of an asymmetric ridge waveguide of Fig. 3. For comparative purpose, we also show the result with the TB approach for the same geometry in Table IV. Since the width of the LB ($2a$) is twice that of the TB in our computation, the convergence characteristics of the TB is better. This is because additional higher modes are needed to obtain convergence as the width $2a$ in region (I) becomes wider. It is interesting to note that the cutoff wavenumbers of the second and third modes in Table IV approximately agree with those of a rectangular waveguide, i.e., 78.54 and 104.7, respectively. In Fig. 9(a), the H_z-field distribution

TABLE III
CUTOFF WAVENUMBERS (IN RADIANS PER METER) OF THE THREE TE MODES FOR AN ASYMMETRIC DOUBLE-RIDGE WAVEGUIDE USING TWO LBS. PARAMETERS: $a^{(1)} = 10$ mm, $d^{(1)} = 10$ mm, $a^{(2)} = 7.5$ mm, $d^{(2)} = 15$ mm, $b = 5$ mm, $T = 45$ mm

Number of modes used	1	4	5
1	37.25	125.4	164.8
3	40.79	137.8	165.2
5	41.06	138.1	165.3
7	41.14	138.2	165.3

TABLE IV
CUTOFF WAVENUMBERS (IN RADIANS PER METER) OF THE FIRST FIVE TE MODES FOR AN ASYMMETRIC DOUBLE-RIDGE WAVEGUIDE USING TWO TBS. PARAMETERS: $a = 5$ mm, $d = 10$ mm, $T^{(1)} = 30$ mm, $b^{(1)} = 20$ mm, $T^{(2)} = 40$ mm, $b^{(2)} = 15$ mm

Number of modes used	1	2	3	4	5
1	40.96	80.36	107.0	137.7	165.3
2	41.15	80.46	107.1	138.2	165.3
3	41.19	80.49	107.2	138.3	165.4
[6]	41.31	80.56	107.2	138.5	165.5

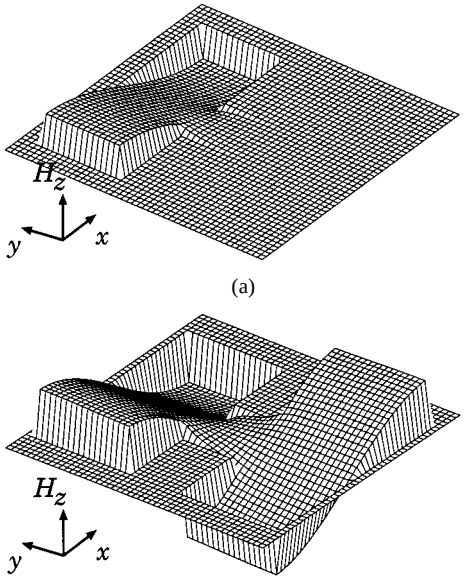

Fig. 9. H_z-field distributions of TE modes using two TBs. (a) Asymmetric double-ridge waveguide. (b) Symmetric double-ridge waveguide.

of the second mode in Table IV is illustrated. The H_z-field is almost concentrated within the left-hand-side cavity of Fig. 3, whose field distribution is very similar to that of a rectangular waveguide. Since the propagation constant for an asymmetric double-ridge waveguide is quite different from the rectangular waveguide similar to the right-hand-side cavity, the wave within the right-hand-side cavity becomes evanescent. The H_z-field plot of a symmetric ridge waveguide is shown in Fig. 9(b). The H_z-field is distributed in two cavities as it should be.

V. Conclusion

A novel TB approach has been proposed for analyzing symmetric and asymmetric ridge waveguides. Simple closed-form dispersion relations for ridge waveguides are expressed in rapidly convergent series. Computed results indicate that, our method, based on a superposition of overlapping TBs, is accurate and numerically efficient. A dominant-mode approximation for a ridge waveguide is shown to be valid and useful for most practical cases. It is possible to extend our theory to the analysis of other complex waveguide structures that can be divided into a superposition of overlapping TBs. For example, the shielded microstrip line, finline, nonradiative dielectric guide, etc., are some typical waveguides that our TB approach can be applied to in order to obtain their dispersion relations.

References

[1] J. P. Montgomery, "On the complete eigenvalue solution of ridged waveguide," *IEEE Trans. Microwave Theory Tech.*, vol. MTT-19, pp. 547–555, June 1971.

[2] Y. Utsumi, "Variational analysis of ridged waveguide modes," *IEEE Trans. Microwave Theory Tech.*, vol. MTT-32, pp. 111–120, Feb. 1985.

[3] A. S. Omar and K. F. Schunemann, "Application of the generalized spectral-domain technique to the analysis of rectangular waveguides with rectangular and circular metallic inserts," *IEEE Trans. Microwave Theory Tech.*, vol. 39, pp. 944–95, June 1991.

[4] W. Sun and C. A. Balanis, "MFIE analysis and design of ridged waveguides," *IEEE Trans. Microwave Theory Tech.*, vol. 41, pp. 1965–1971, Nov. 1993.

[5] S. Amari, J. Bornemann, and R. Vahldieck, "Application of a coupled-integral-equations technique to ridged waveguides," *IEEE Trans. Microwave Theory Tech.*, vol. 44, pp. 2256–2264, Dec. 1996.

[6] V. A. Lenivenko, "Propagation characteristics of asymmetric double ridge waveguide," in *Asia–Pacific Microwave Conf.*, 2000, pp. 1235–1237.

[7] Y. H. Cho and H. J. Eom, "Fourier transform analysis of a ridge waveguide and a rectangular coaxial line," *Radio Sci.*, vol. 36, no. 4, pp. 533–538, July–Aug. 2001.

[8] I. V. Petrusenko, A. B. Yakovelev, and A. B. Gnilenko, "Method of partial overlapping regions for the analysis of diffraction problems," *Proc. Inst. Elect. Eng.*, pt. H, vol. 141, pp. 196–198, June 1994.

[9] A. B. Gnilenko, A. B. Yakovlev, and I. V. Petrusenko, "Generalized approach to modeling shielded printed-circuit transmission lines," *Proc. Inst. Elect. Eng.*, pt. H, vol. 144, pp. 103–110, Apr. 1997.

[10] P. Lampariello and A. A. Oliner, "New equivalent networks with simple closed-form expressions for open and slit-coupled E-plane tee junctions," *IEEE Trans. Microwave Theory Tech.*, vol. 41, pp. 839–847, May 1993.

[11] R. E. Collin, *Field Theory of Guided Waves*, 2nd ed. New York: IEEE Press, 1991, pp. 72–78.

[12] B. T. Lee, J. W. Lee, H. J. Eom, and S. Y. Shin, "Fourier-transform analysis for rectangular groove guide," *IEEE Trans. Microwave Theory Tech.*, vol. 43, pp. 2162–2165, Sept. 1995.

Yong H. Cho was born in Daegu, Korea, in 1972. He received the B.S. degree in electronic engineering from the Kyungpook National University, Daegu, Korea, in 1998, the M.S. degree in electrical engineering from the Korea Advanced Institute of Science and Technology (KAIST), Daejeon, Korea, in 2000, and is currently working toward the Ph.D. degree in electrical engineering at KAIST.

His research interests include the dispersion and coupling characteristics in waveguides and transmission lines.

Hyo J. Eom (S'78–M'81–SM'99) received the B.S. degree in electronic engineering from the Seoul National University, Seoul, Korea, in 1973, and the M.S. and Ph.D. degrees in electrical engineering from the University of Kansas, Lawrence, in 1977 and 1982, respectively.

From 1981 to 1984, he was a Research Associate with the Remote Sensing Laboratory, University of Kansas. From 1984 to 1989, he was a faculty member of the Department of Electrical Engineering and Computer Science, University of Illinois at Chicago. In 1989, he joined the Department of Electrical Engineering, Korea Advanced Institute of Science and Technology (KAIST), Daejeon, Korea, where he is currently a Professor. His research interests are wave diffraction and scattering.